Quantitative analysis of trace OH in garnet and pyroxenes

DAVID R. BELL,* PHILLIP D. IHINGER,** GEORGE R. ROSSMAN

Division of Geological and Planetary Sciences, California Institute of Technology, Pasadena, California 91125, U.S.A.

ABSTRACT

To calibrate infrared (IR) spectroscopy for quantitative analysis of trace structural OH in specific minerals, we have determined concentrations of H in pure separates of mantle-derived pyrope garnet (56 ± 6 ppm H_2O by weight), augite (268 ± 8, ppm H_2O), and enstatite (217 ± 11 ppm H_2O) by manometry after heating the samples and extracting H_2 gas under vacuum. IR spectroscopy confirmed the presence of intrinsic OH in these samples prior to extraction and indicated between 86 and 100% removal of H during the extraction procedure. The integral specific absorption coefficients of 1.39 ± 0.14 (1σ), 7.09 ± 0.32, and 15.6 ± 0.94 /(ppm $H_2O \cdot cm^2$) for pyrope, augite, and enstatite, respectively, allow precise spectroscopic determination of the OH content of upper mantle garnets and pyroxenes to concentration levels of a few parts per million. Uncertainties in accuracy depend on mineral composition and characteristics of the OH absorption spectrum and are estimated to range between ±10 and ±50%.

INTRODUCTION

Trace quantities of hydroxyl (OH) have been detected spectroscopically in many minerals that are supposedly anhydrous (Rossman, 1988). This form of H is thought to influence mechanical and other physicochemical properties of silicate materials (e.g., Mackwell et al., 1985) and appears to be a significant "water" reservoir in the Earth's mantle (Bell and Rossman, 1992a). Quantitative analysis of trace H is therefore desirable for a proper understanding of its role in geological processes. Infrared (IR) absorption spectroscopy is a highly sensitive, site-specific, nondestructive method for the study of OH in minerals and with appropriate calibration can provide accurate and precise quantitative analysis of trace OH. In this study, we used vacuum extraction and manometry to measure the H contents of spectroscopically characterized clinopyroxene, orthopyroxene, and garnet samples of high purity. The results are used to calibrate the IR spectra for quantitative analysis of structurally bound OH in these minerals, which are important phases in the upper mantle.

Quantitative IR spectroscopy

Paterson (1982) has summarized a methodology for quantitative IR analysis of OH in minerals and here we follow the terminology used in that paper. Equation 1 is a modified integral form of the Beer-Lambert law for determining the concentration of an oriented, absorbing species, such as an OH group, from the IR spectrum of a mineral:

* Present address: Geophysical Laboratory, 5251 Broad Branch Road NW, Washington, DC 20015-1305, U.S.A.

** Present address: Department of Geology and Geophysics, Yale University, New Haven, Connecticut 06511, U.S.A.

$$c = \frac{1}{I\gamma} \int_{\nu_1}^{\nu_2} K(\nu) \, d\nu. \tag{1}$$

In Equation 1, c is the concentration of the absorbing species (e.g., OH), conventionally expressed as moles of solute per liter of host phase, and $K(\nu)$ is the absorption coefficient (absorbance per unit thickness) of the OH as a function of wavenumber (ν) and implies the prior subtraction of the absorption due to the host phase (the baseline). Because the IR absorption spectra of OH in anhydrous minerals are commonly complex, with multiple unresolved bands, the integrated absorption coefficient, $\Delta = \int K(\nu) \, d\nu$ is usually a more convenient measure of absorption intensity per unit thickness than linear absorbance (A). The term γ is an orientation factor discussed by Paterson (1982), and is introduced to account for various possible mineral and OH vector orientations and polarization of the IR beam. I is the integral (or integrated) molar absorption coefficient, which is a measure of the efficiency of light absorption and which depends on the compositional and structural properties of the material and the transition in question. Although the need for the determination of I or ϵ (the molar absorption coefficient) for specific materials was recognized early (e.g., Scholze, 1960), accurate evaluation of these parameters has proved problematic for H-poor materials because of the difficulty of performing independent analyses of H at the trace level. In addition, the calibrations that have been performed have allowed very little evaluation of the uncertainties in the precision or accuracy in the values reported because the methods and sample characteristics were rarely described in any detail.

As an alternative to mineral-specific calibration, Paterson (1982) proposed a method for estimating ϵ or I for unknown samples from the systematics in the relation-

TABLE 1. Compositions and densities of minerals used in this study

	Clinopyroxene (3) PMR-53	Orthopyroxene (8) KBH-1.opx	Garnet (3) MON-9	Garnet (3) KM-1493
SiO_2	54.78	54.68	42.20	40.99
TiO_2	0.35	0.11	1.25	0.62
Al_2O_3	2.83	4.73	20.39	22.87
Cr_2O_3	0.14	0.49	0.62	n.d.
FeO^*	6.87	5.88	10.89	13.54
MnO	0.14	0.14	0.28	0.39
MgO	18.30	32.92	19.52	16.34
CaO	13.26	0.86	4.62	5.55
Na_2O	2.13	0.12	0.11	0.03
K_2O	0.05	n.d.	n.a.	n.a.
NiO	0.07	0.10	0.01	n.a.
P_2O_5	n.a.	n.a.	0.05	0.03
Total	98.92	100.03	99.93	100.36
$D \pm 2\sigma$	3.339 ± 0.017	3.318 ± 0.017	3.730 ± 0.014	

Note: PMR-53 = augite megacryst, 3 × 2 × 2 cm, from kimberlite, Premier Mine, South Africa. KBH-1.opx = aluminous enstatite mineral separate, 1–5 mm, from anhydrous type I (Frey and Prinz, 1978) spinel lherzolite, Kilbourne Hole basanite maar, New Mexico. MON-9 = pyrope garnet megacryst from kimberlite, Monastery Mine, South Africa. Similar samples described by Nixon and Boyd (1973) and Gurney et al. (1979). KM-1493 = pyrope garnet megacryst from alkali basalt, Kerem Maharal, Mount Carmel, Israel. Numbers in parentheses refer to number of analyses averaged; n.a. = not analyzed; n.d. = not detected.
* All Fe as FeO.

ship between the absorption coefficient and frequency of a variety of substantially hydrous materials and compounds. This calibration, which has been applied often in studies of OH in quartz and olivine, was not necessarily intended for rigorously accurate, quantitative infrared analysis of all forms of OH, but rather as a workable general formula for semi-quantitative analysis (Paterson, 1982). There is considerable scatter of data points about the best-fit line used by Paterson in relating ϵ to ν, and indeed no a priori reason to expect anything better than a broad data array following the general principle that an increase in wavenumber leads to an increase in absorption intensity (Ikawa and Maeda, 1968). Direct calibrations of OH-bearing minerals (Scholze, 1960; Rossman and Aines, 1991; Skogby and Rossman, 1991; Pawley et al., 1993) indicate deviations of up to a factor of three from molar absorption coefficients calculated from Equation 4 of Paterson (1982). It therefore appears that accurate spectroscopic analysis of OH in minerals requires overcoming the difficulties of independent calibration analysis of the specific minerals of interest.

Previous calibrations of OH in garnet and pyroxenes

The improved analysis of small quantities of H in materials is a continuing effort, complicated by the ubiquity of water and other H-bearing phases as contaminants in the laboratory and as agents of alteration in nature. Aines and Rossman (1984a) used coulometric, gravimetric, and manometric techniques to determine the H_2O contents of selected garnets of different composition. The analyzed H_2O contents ranged from 0.06 to 0.36 wt% with corresponding molar absorption coefficients ranging over nearly two orders of magnitude. We now recognize that these

analyses probably overestimated the true OH contents. The application of nuclear reaction techniques (e.g., Rossman et al., 1988) has resulted in lower estimates of the OH contents of these garnets, but there is still considerable scatter in the data (Rossman, 1990). One of the causes of this scatter may be the vastly different spectroscopic characteristics of OH in the different samples. In some garnet groups, e.g., the grossular garnets, spectral differences even occur in samples of similar composition (Aines and Rossman, 1984a; Rossman and Aines, 1991). Initial efforts using this technique to measure H in pyrope garnets were unsuccessful because of the low concentrations of H (Rossman et al., 1988). Calibration of the OH bands in pyroxenes by nuclear reaction analysis has been reported in Skogby et al. (1990). Advances in the development of low-background detector systems for this technique (Kuhn et al., 1990; Endisch et al., 1994) and the continuing refinement of ion microprobe techniques (Deloule et al., 1991; Kurosawa et al., 1992, 1993) hold promise for the future.

SAMPLE DESCRIPTION

One of the greatest obstacles to accurate bulk analysis of low concentrations of H in materials is the presence of trace amounts of contaminant hydrous phases in, or on, the samples themselves. For anhydrous minerals with H_2O concentrations of at most a few hundred parts per million, the absence of traces of hydrous phases in the analyzed aliquot is critical for accurate analysis. This places a high priority on appropriate sample selection. The samples used in this study were selected for their large size, homogeneity, and high degree of purity, combined with relatively high OH content. An important factor in the successful sample preparation was the existence of large volumes (~0.05–0.1 cm^3 in the garnet and augite) of apparently flawless mineral in the starting materials, which facilitated the efficient separation of host mineral from contaminants. The clinopyroxene and garnet were single megacrysts, whereas the orthopyroxene was a composite of grains separated from a single lherzolite xenolith.

Details of sample provenance and composition are given in Table 1. Both garnet samples are pyrope, with the sample from the alkali basalt being somewhat more Fe-rich. The clinopyroxene is classified as an augite in the scheme of Morimoto et al. (1988) but is notably subcalcic and relatively Fe-poor compared with common augite in crustal rocks. The orthopyroxene is an aluminous enstatite typical of mantle-derived spinel peridotite xenoliths in basalt.

In these samples, the contaminant H-bearing phases are largely restricted to linings of cracks that traverse the samples in abundance. In the case of garnet and clinopyroxene, some of this material may be derived from the host kimberlite and probably includes serpentine. Apart from the visually obvious mineral-lined cracks, finer scale fractures also occur, the surfaces of which are either visually free of a lining material or are plated with a very thin calcite veneer.

The outer surfaces of the orthopyroxene grains that represent original mineral grain boundaries have a clear to lightly frosted appearance, but microscopic examination of the surfaces revealed a typical absence of other mineral phases. Large inclusions of clinopyroxene, spinel, and olivine (the primary coexisting phases in the lherzolite nodule) were sometimes observed in the orthopyroxene mineral grains, and all inclusion-bearing grains were excluded from the analyzed aliquots. Examination of selected gemmy areas of the minerals under the optical microscope (400×) revealed no further evidence of inclusions.

METHODS

Sample preparation

To ensure extremely pure mineral fractions for the H extraction, two preparation methods were employed. For the orthopyroxene KBH-1, conventional hand-picking techniques were applied. Mineral grains could be separated from one another by hand or with gentle crushing because the xenolith was unusually friable. This commonly caused the grains to separate along natural grain boundaries. The orthopyroxene grains were then individually hand-picked under a binocular microscope in air. This separate was washed in distilled water, washed again in warm dilute HCl in an ultrasonic bath, and rinsed in distilled water. The clean separate was then reexamined under a binocular microscope using large area illumination from below and with polarizers in extinction. The mineral grains were immersed in ethanol, and each grain was examined for the presence of cracks, fine fractures (line or not lined with minerals), foreign inclusions, or surface phases. The features were well illuminated, especially when the mineral grain was manipulated into an extinction orientation. Only grains free of all these features were retained for analysis. Large grains that were rejected on the first and second passes but with minimal contamination were lightly crushed, washed, and reexamined. This crushing treatment yielded additional clean grains. The final clean separate was washed in ethanol, dried, weighed into three mass fractions, and stored in glass vials.

The megacryst samples were treated differently. Each sample (a single crystal) was sliced into several wafers using a diamond saw. The wafers measured ~1 mm in thickness, depending on the transparency of the sample, and typically 2 cm in diameter. In many cases, especially for the thicker wafers, the wafers were then doubly polished. A wafer from each sample was set aside for core-to-rim homogeneity testing. The wafers were then broken along preexisting cracks to yield platelets (maximum dimension 3–12 mm) with gemmy interiors and thin margins consisting of minerals that had lined the fractures. These margins were then ground off with a diamond-impregnated Ni grinding wheel so that each platelet was entirely bounded by fresh (i.e., artificially generated in the laboratory) surfaces. Each platelet was then examined under the binocular microscope and those entirely free of cracks, inclusions, or foreign phases were set aside. Platelets with minimal contamination were rebroken and reground, or the offending marginal material together with a selvage of pure mineral were chipped off with the aid of forceps under the binocular microscope. The clean material was then crushed to a diameter of ≤2 mm in the case of the garnet and the fraction <100 μm in size was discarded to minimize adsorbed H_2O. Most sample mass was contributed by grains <1 mm in diameter. The crushed, sieved, and rewashed garnet was then examined in the binocular microscope under ethanol, and any visible foreign material was removed. In the case of the clinopyroxene samples, only the thickest plates were reduced in size by gentle crushing. In all samples, large grain size was deliberately maintained to minimize the surface to volume ratio. The trade-off with increased diffusion distance resulted in some fraction of the intrinsic OH being retained after extraction, particularly in the coarsest fragments (see below). After a final cleaning in ethanol and isopropanol, the samples were weighed and stored.

Infrared spectroscopy

Samples for IR spectroscopy were oriented using a petrographic microscope, sometimes with the aid of a spindle-stage attachment, and doubly polished plates were prepared with alumina grit. The anisotropic materials typically required two orthogonal plates to yield spectra in all three principal vibration directions of the optical indicatrix. The sample orientation procedure does not always yield plates that are perfectly perpendicular to a principal vibration direction. We estimate that these deviations from the ideal orientation may be as great as 10° and result in discrepancies between measured and true absorptions of up to 5% in any particular orientation. These differences are reduced when all three vibration directions are summed because of the orthogonality of the vibration directions for any one plate. If all three directions are measured on a single mineral fragment (i.e., with two orthogonal sets of surfaces), then the discrepancy is reduced further because the surfaces are typically very close to within 90° of one another (90 ± 5°).

Sample thickness was measured with an electronic micrometer with a reproducibility of ±0.001 mm. However, it was not always possible to generate perfectly parallel mineral plate surfaces, and the errors introduced by slight wedging result in an uncertainty in sample thickness of about ±0.002 mm. The thickness of the samples analyzed in this study ranged from about 0.5 to 2 mm, so that errors introduced by the thickness measurement rarely contribute as much as 1% (relative).

IR spectra were obtained using the method described by Skogby et al. (1990) and Bell and Rossman (1992b). In order to establish the homogeneity of the garnet and clinopyroxene samples, spectra were collected at several points on selected large doubly polished wafers. Homogeneity of the orthopyroxene sample was checked by analyzing five separate oriented grains.
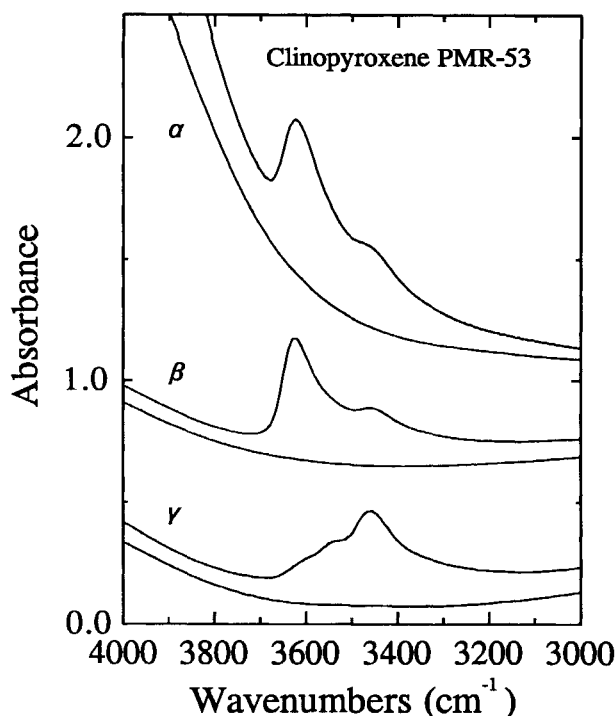
Fig. 1.   Infrared spectra of OH in clinopyroxene PMR-53 with E polarized parallel to α, β, and γ. The upper spectrum in each orientation is the untreated sample, the lower spectrum is after extraction at ~1000 °C for 3 h and at 150 °C < T < 900 °C for 2.5 h. Spectra normalized to 1 mm thickness.

The infrared absorption spectra of the fundamental OH stretching vibration in the minerals studied here are composed of many partially overlapping bands (Figs. 1–3). These are superimposed on a baseline with contributions from electronic transitions (here owing to Fe^{2+}) as well as Si-O vibrations. The precise location of this background (baseline) absorption is the source of the greatest uncertainty in determining the net OH absorbance. This is discussed further in Appendix 1. In this study, the baselines for orthopyroxene and garnet were obtained from the spectra of the totally dehydrated minerals prepared by heating the samples at 1000 °C in air (Fig. 2). For the clinopyroxene, some change in the character of the 4300 cm^{-1} Fe^{2+} (M2) band occurred after heating, and in this mineral the background was estimated visually with due reference to the dehydrated sample.

In order to determine the individual band absorbances that contribute to the broad absorption spectra of OH in these minerals, we attempted to model the spectra mathematically using a Gaussian and Lorentzian peak-fitting routine. This procedure was abandoned once its arbitrariness became apparent; that is, good fits to the spectra were attained only when the number of input bands exceeded the number of visible peaks in the spectrum. While it is probable that unresolved peaks do occur in these spectra, the positions of the extra hidden peaks in the spectrum could not be independently verified or predict-
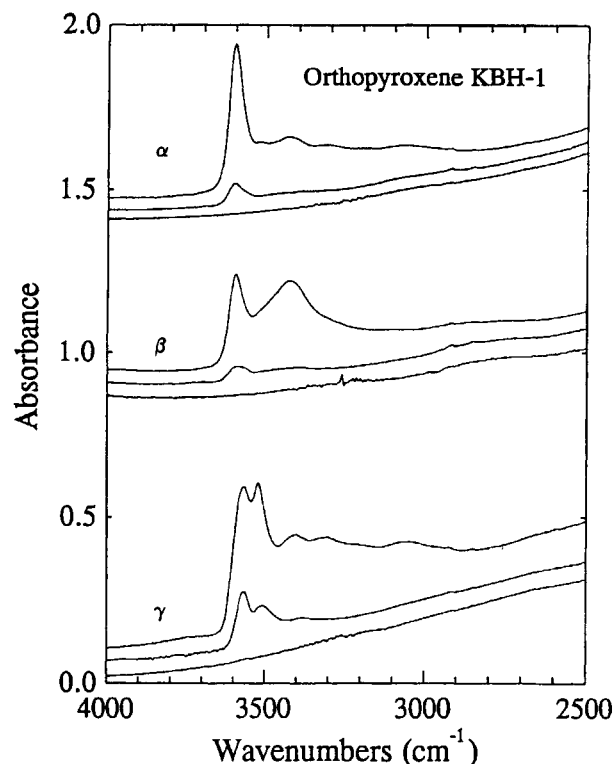

Fig. 2.   Infrared spectra of OH in orthopyroxene KBH-1.opx with E polarized parallel to α, β, and γ. The upper spectrum in each orientation is the untreated sample before extraction, the middle spectrum is after extraction at ~1000 °C for 3.25 h and at 150 °C < T < 900 °C for 1.5 h. The minimum dimension of sample before polishing was 0.71 mm. The β and γ spectra taken in direction parallel to thickness (0.71 mm), the α spectrum taken parallel to sample length (1.54 mm). The lower spectrum in each orientation is the same fragment heated in air for 24 h at 1000 °C and is, as far as can be detected, OH-free. Subtraction of this lower spectrum from the upper two was used to determine the OH integrated absorbance in those samples. All spectra normalized to 1 mm thickness.

ed a priori and were thus not considered reliable. In lieu of an appropriate resolution of the component bands in the spectra, the total absorbance in these minerals was determined by summing the absorbances at intensity maxima in the spectra (Table 2). In reality, the molar absorption coefficients appropriate to these frequencies are expected to differ from one another, and should ideally be determined separately as the calibrations are refined.

The OH-band intensities and integrated absorbances derived from the IR spectra are given in Table 2. The errors reported in Table 2 include all sources of uncertainty for orthopyroxene and garnet because they are derived from the statistics for measurements on multiple samples.

Manometry

The technique of gas extraction and manometric measurements is standard in the preparation of samples for

H isotopic analysis and has been described by Epstein and Taylor (1970) and Newman et al. (1986). Samples were loaded in air into a large Pt crucible that had been outgassed overnight at ~1100 °C, covered with a Pt lid, placed into a glass heating vessel, and attached to the vacuum line. It was noted that despite the overnight degassing step, the cleaning of residual glass from the crucible with HF increased the blank. Thus, with the exception of sample KM1493, a single Pt crucible was reused without any cleaning procedure. The sample was heated with an induction furnace. Results of previous attempts of temperature calibration using a thermometer, optical pyrometry, and melting point determinations for several metals suggest a temperature uncertainty of ~100 °C at high temperatures. H species were converted to H_2O over hot CuO, followed by cryogenic separation from other gases. H_2O was converted to H_2 by reaction with U at 700 °C (Bigeleisen et al., 1952). The H_2 was collected with a Hg Toepler pump and its volume was measured in a Hg manometer with a reproducibility of ±0.1 μmol. The manometer was previously calibrated by measuring the height of the Hg column for known amounts of CO_2 gas under room-temperature conditions.

A two-stage heating procedure was used in the extraction of H from all samples. Each aliquot was initially held at ~150–200 °C for 3 h to remove adsorbed H_2O from the surface of the sample without releasing structurally bound H. The precise temperature could not be determined because of the induction method of heating. We are confident that no intrinsic OH was lost from the samples in this temperature range because spectroscopically monitored heating experiments in air and vacuum demonstrated the onset of intrinsic H loss from the minerals at temperatures of ≥500 °C. The H-bearing gas that evolved during this low-T step was mostly H_2O. The second heating step involved stepwise elevation of the temperature to that slightly below the sample's melting point. We chose not to melt the samples because of the greater diffusion distances for the coalesced mass, the possibility of trapping bubbles in the viscous melt, and the loss of
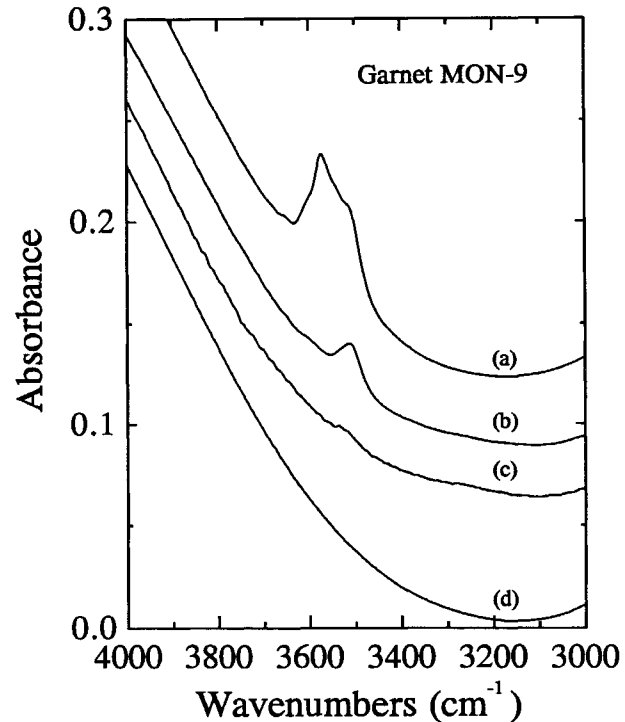

Fig. 3. Unpolarized IR spectra of garnet MON-9 in the OH-stretching region between 3000 and 4000 cm^{-1}. (a) Untreated sample before extraction. (b) Garnet MON-9 after extraction at ~900 °C for 10 h. Sample thickness before polishing was 0.95 mm. (c) Garnet MON-9 after extraction at ~900 °C for 32 h. Representative of samples 0.3–1.5 mm thick before polishing. (d) Garnet MON-9 with all detectable OH removed after heating for 24 h in air at 1000 °C. All spectra normalized to 1 mm thickness.

the ability for direct comparison of "before" and "after" IR spectroscopic measurements of OH. Pyroxene samples were heated to ~1100 °C, whereas garnet was heated to ~900 °C because this mineral melts at the higher temperatures. Although the temperature was raised incre-

TABLE 2. Infrared spectroscopic data

Mineral	ν (cm^{-1})	Band intensity (A/cm)			ΣA^*	Δ/cm before extraction	Δ/cm after extraction	Δ/cm extracted OH
		α	β	γ				
Clinopyroxene	3625	4.09**	6.54**	—				
PMR-53	3540	—	—	1.94**	15.72 ± 0.43	1903 ± 69	0	1903 ± 69
	3460	1.36	1.43	3.18**				
Orthopyroxene	3600	4.56**	3.03**	—				
KBH-1.opx	3570	—	—	4.23**				
	3520	1.44**	—	4.18**				
	3430	1.48**	2.65**	—	30.49 ± 0.69	3221 ± 105	461 ± 23	2760 ± 108
	3410	—	—	2.31**				
	3300	1.03**	1.32**	1.91**				
	3060	0.60**	0.55**	1.22**				
Garnet MON-9	3571		0.621 ± 0.006**†		1.119 ± 0.007	77.3 ± 1.3	—	~77.3 ± 1.3
	3512		0.499 ± 0.006**†					

Note: all intensities (absorbances) and integrated absorbances (Δ) are per centimeter thickness. Errors represent 1σ.
* Bands included in the summed intensity are a matter of choice.
** Summed bands, which are the most prominent bands in the OH spectrum.
† Absorbance for garnet determined with unpolarized IR beam in random crystallographic direction.
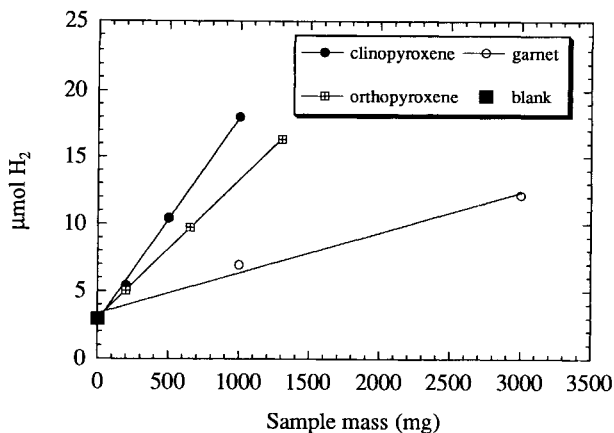
Fig. 4. Yields of H_2 (determined by manometry) as a function of aliquot mass of sample for the high-temperature step (greater than ~150 °C) in the three minerals garnet MON-9, enstatite KBH-1.opx, and augite PMR-53, as well as a blank (empty Pt crucible). The point corresponding to the greatest mass of garnet (~3 g) is the sum of the yields for the two repeated extractions on the same sample minus the blank value of 2.97 μmol H_2 (the plotted yield therefore includes the contribution from one procedure blank rather than two). Uncertainties of measurement in mass and μmol H_2 are smaller than the plotted symbols. The lines shown for each mineral are the linear regression of the data points and the blank. The concentrations reported in Table 3 are derived from the slopes of these lines.

TABLE 3. Manometry data

| Mineral sample | Aliquot mass (mg) | H yield (μmol) | | H_2O ppm (wt)* |
		Low T	High T	
Clinopyroxene	200.0	1.38	5.43	
PMR-53	497.2	3.10	10.44	268 ± 7.5
	1024.6	4.02	18.03	
Orthopyroxene	200.1	1.64	5.06	
KBH-1.opx	645.6	3.00	9.76	186 ± 1.4**
	1299.8	4.12	16.38	
Garnet MON-9	1000.4	4.48	6.95	
	3000.0	4.30	11.16	55.7 ± 5.5
	2800.0†	4.84	3.96	
KM-1493‡	1799.0	4.49	4.79	<1§
Blank	0.0	1.13	2.97	

* Uncertainty in parts per million calculated from the regression statistics and represents 1σ.
** Concentration of the extracted H. Original concentration is 217 ± 11 ppm.
† The 3000 mg fraction of MON-9 was crushed and re-analyzed after IR analysis following the first heating showed residual OH. In the process, 200 mg was lost as fines (<100 μm).
‡ Blank levels were higher for this determination owing to a different analytical procedure.
§ Determined by IR spectroscopy (Bell and Rossman, 1992b).

mentally and the proportions of evolved H_2O to H_2 were monitored at intermediate temperatures, all H aliquots from temperatures greater than ~150–200 °C (a specific setting on the power control dial) were combined for manometry. In contrast to the low-temperature fraction of evolved gas, the dominant H-bearing species released during the high-temperature step was H_2. The length of this step varied from 6 h for orthopyroxene to 30 h in total for garnet.

A blank determination was performed by measuring the H_2 that evolved from an empty crucible, following the same preparation procedures, after a 5.5 h high-T heating step. This yielded 2.97 μmol H_2.

RESULTS

Infrared spectroscopy

IR spectra for the three minerals are illustrated in Figures 1–3. The IR spectra of OH in the clinopyroxene (Fig. 1) resemble those of augite described by Skogby et al. (1990). Both augite and diopside display peaks near 3630, 3530, and 3460 cm^{-1} (Ingrin et al., 1989; Skogby et al., 1990), but augite (and our clinopyroxene sample) lacks the diopside band near 3350 cm^{-1}. The orthopyroxene OH spectra (Fig. 2) differ somewhat from previously published examples, although several bands identified by Beran and Zemann (1986) and Skogby et al. (1990) are present. The IR spectrum of OH in the garnet megacryst (Fig. 3) is similar to those described by Aines and Rossman (1984a, 1984b), but displays a peak at 3512 cm^{-1},

a typical feature of Ti-bearing mantle garnets (Bell and Rossman, 1992b).

IR spectra of samples taken after H extraction are also shown in Figures 1–3. Figures 2 and 3 show that most, but not all, of the intrinsic OH was removed from the orthopyroxene and garnet samples. No residual OH was detected in the clinopyroxene (Fig. 1). Because garnet was analyzed at the lowest temperature and an initial 15 h extraction still left significant OH in the thickest grains, the 3000 mg sample was subjected to a second extraction after crushing of the largest grains. Typical differences between the OH contents of garnets from these extractions are shown in Figure 3. IR analysis of a series of grains of different original thickness confirmed that the smallest grains lost a greater proportion of OH than did the larger ones during the extraction, presumably because of the greater diffusion distances for the latter. This residual OH has not been taken into account in the calculation of the molar absorption coefficient for garnet because of its small magnitude (Fig. 3) and because of the uncertainties in accurately quantifying this amount. It was found that the dominant OH band at 3570 cm^{-1} is quite easily removed during extraction, whereas the usually less intense 3512 cm^{-1} band is far more stable at high temperatures. This same behavior has been observed during heating experiments on garnets in air and suggests the presence of at least two distinct OH sites in these garnets. A quantitative assessment of the remaining fraction of OH in the orthopyroxene (14%) is reported in Table 2 and is based on the assumption that the one sample analyzed is representative of the whole batch after extraction. This is an oversimplification because of the distribution of grain sizes. In reality, this estimate for residual OH is probably high because the grain chosen for IR analysis was one of the larger fragments in the extracted sample.

TABLE 4. Molar and specific absorption coefficients for OH* in pyrope garnet, enstatite, and augite calculated from the data in Tables 1, 2, and 3

	Clinopyroxene PMR-53	Orthopyroxene KBH-1	Garnet MON-9
ϵ [L/(mol·cm)]	316 ± 12	734 ± 21	96.9 ± 9.6
ϵ' [1/(ppm·cm)]	0.0586 ± 0.0023	0.135 ± 0.004	0.0201 ± 0.0020
I [L/(mol·cm²)]	38300 ± 1700	80600 ± 3200	6700 ± 670
I' [1/(ppm·cm²)]	7.09 ± 0.32	14.84 ± 0.59	1.39 ± 0.14

Note: ϵ = molar absorption coefficient; ϵ' = specific absorption coefficient; I = integral molar absorption coefficient; I' = integral specific absorption coefficient. All coefficients normalized to 1 cm sample thickness. Absorption coefficients for the pyroxenes are for linearly polarized light, with absorptions in all three orthogonal principal vibration directions summed (γ = 1). Note that values for ϵ and ϵ' are specifically for the bands summed as indicated in Table 2. Absorption coefficients for garnet are based on unpolarized radiation in one direction only and must be multiplied by three in order to be compared in a physical sense with the pyroxene values (i.e., compare I/γ in all cases). Uncertainties reported are ±1σ and are derived by propagation of errors (see Appendix).
   * OH concentration expressed as moles H_2O per liter mineral (ϵ and I) or as parts per million H_2O by weight (ϵ' and I').

Manometry

The amount of H_2 extracted in the high temperature (>150–200 °C) treatment of each sample is reported in Table 3 and plotted as a function of aliquot mass in Figure 4. The data display excellent correlations between H yield and sample mass for each mineral studied, which is an indication of both the homogeneity of the sample splits and the reproducibility of the blank present in each extraction (3 μmol). Furthermore, the consistency of the results indicates that the small amounts of residual OH after extraction (Figs. 1–3 and Table 2) do not disrupt the correlation. The residual OH is taken into account in the calculation of the total OH content of the orthopyroxene but not in that of the garnet. It is apparent that the differential degrees of incomplete degassing that must occur for the range of thicknesses of orthopyroxene and garnet mineral fragments have not affected the overall yield of each aliquot to substantially different degrees. We are also confident that the positive correlations shown in Figure 4 are not due to adsorbed material on the fragment surfaces that is stable to temperatures in excess of 150 °C. This is precluded by the manometric analysis of 1800 mg of the garnet KM-1493, which was found by IR spectroscopy to be extremely poor (<2 ppm) in OH. This sample was contained in an HF-treated crucible that produced somewhat higher blanks (see above) but still yielded only 4.9 μmol of H_2 (including blank of >3 μmol). It would be predicted that this sample would yield considerably more H_2 (at least 9 μmol) if all the high-temperature H_2 was derived from adsorbed material that was proportional in quantity to the sample mass. The possibility of surface contamination was further tested by subjecting a garnet aliquot used in the extraction procedure to a second acid wash and cleaning in organic solvents (acetone, ethanol, and isopropanol). This retreated aliquot was run through the extraction procedure again and yielded a high-T H_2 concentration comparable to blank level, demonstrating that grain surface residues from the organic solvents are not the cause of the measured H_2.

The estimates of the concentrations of OH (expressed as parts per million H_2O) in the minerals were derived by linear regression of the data in Figure 4 (including the blank datum in each regression) and are listed in Table 3 with the associated uncertainties derived from the errors in the slope of the regression lines in Figure 4. These data have been combined with the IR spectroscopic data from Table 2 to calculate a set of molar and specific absorption coefficients (Table 4). The integrated absorbances for the anisotropic minerals have been calculated as the sum of the integrated absorbances in the three principal vibration directions per centimeter of sample thickness. The linear absorbances have been calculated with the procedure of Skogby et al. (1990) and Table 2, but with the exception that our values are for H_2O rather than OH. The ramifications of these procedures are further discussed below.

The conversion from the measured concentration of micromoles H_2O per gram of mineral to the conventional units of ϵ of liters per mole requires an estimate of the density of the mineral. We have determined the density of our mineral samples by repeated weighing of pure, gem-quality fragments in air and toluene. The densities and their associated uncertainties are reported in Table 1. However, for general application we prefer to express the absorption coefficient as a factor relating absorbance per centimeter of sample thickness to H_2O concentration in weight percent (see Rossman et al., 1988). This circumvents the troublesome density determination and reports concentrations in units more commonly used in geology.

Discussion

The origin of the extracted H_2

As discussed above, the primary concern of this study has been the elimination of contaminating hydrous materials from our samples. Several lines of evidence suggest that the measured H_2 is derived from the breakdown of OH groups within the sample mineral structure and does not originate from other phases, which may have been present as unseen inclusions or imperfections within the mineral grains.

The first line of evidence is that the spectroscopic data show that 86% or more of the intrinsic OH has been removed from the samples. The H_2 yields are of the range

of magnitude expected from the intrinsic component on the basis of recent results from nuclear reaction analysis of the same samples (D. Endisch et al., in preparation). In fact, the sample aliquot sizes were selected so that predicted H_2 yields would provide sufficient signal-to-noise ratio, given the known blank levels of the manometric technique. Second, analysis of a garnet sample with low intrinsic OH content, the megacryst KM-1493 with <2 ppm H_2O (on the basis of IR), yielded a predictably low amount of H_2, close to the blank level for that procedure. Furthermore, we observe that the gas evolved during the low-temperature heating step is predominantly H_2O, whereas that evolved at high temperatures is predominantly H_2. Potential hydrous contaminant minerals precipitated at low temperatures may be expected to dehydrate and release H_2O at low temperatures. In contrast, the high-temperature component is consistent with the progressive dehydrogenation (prior to dehydration) of Fe-bearing minerals with relatively high thermal stabilities (e.g., Vedder and Wilkins, 1969; Phillips et al., 1988). Some CO_2 was observed in the gas fraction of both high- and low-temperature steps (after oxidation of the evolved gases in the CuO furnace), but unfortunately our procedure did not permit us to distinguish between CO_2 derived from oxidized C and that derived from reduced C. Thus, it is possible that some calcite contaminant was introduced with the sample, but this would not influence the amount of H measured. Contribution of H from traces of solid hydrocarbons such as those observed by Tingle et al. (1990) and discussed by Mathez (1987) cannot be precluded, other than to emphasize the efforts made to avoid such material during hand-picking by excluding cracked grains.

We believe that most of the blank-corrected H_2 measured by manometry is derived from the spectroscopically observed, structurally bound OH within the mineral samples. The argument is weakest in the case of garnet, where sample masses are highest, measured concentrations of H do not differ by more than a factor of three from blank levels, and analytical consistency is poorest. The probability of a small proportion of H contamination from phases that escaped notice must be admitted, particularly in the case of garnet. In such cases the calibrations determined here place lower limits on the molar and specific absorption coefficients listed in Table 4.

Comparison with previous work

Mineral-specific calibrations. Our estimate of $I = 6700$ L/(mol·cm²) for garnet would result in spectroscopically determined H_2O contents lower by a factor of 20–25 than estimates using the Aines and Rossman (1984a) calibration on garnets of similar composition. However, our result is in reasonable agreement with their value of 8000 L/(mol·cm²) determined by both coulometry and manometry for a grossular with 0.18 wt% H_2O. We believe that the discrepancy in the low-OH pyropes most likely arises from impurities in the samples used in that study and from instrumental limitations caused by baseline drift

in the thermal gravimetric analysis instrument. Our calibration is within error of the mean integral molar absorption coefficient of 7070 ± 1030 L/(mol·cm²) for seven grossular garnets calculated from the data of Rossman and Aines (1991). Nuclear reaction analyses for pyrope-almandine garnets reported by Rossman (1990) display a general positive correlation with infrared peak intensity, but with considerable scatter. Arbitrarily ignoring two aberrant points and assuming a constant density of 3.85 g/cm³, a best-fit line through this data set gives $\epsilon = 15$ L/(mol·cm), compared with 97 L/(mol·cm) (this study). Uncertainties in the influence of surface effects, corrections for introduced impurities, and the possibility of H migration during nuclear reaction analysis cause us to favor the manometric calibration.

In order to compare our clinopyroxene calibration with that reported by Skogby et al. (1990) for augite (Table 4), we have summed the intensities of the bands at 3600, 3520, and 3460 cm⁻¹ as shown in Table 2. The ϵ values agree within error, promoting confidence in the calculation of the H contents of augitic pyroxenes. One of these analyses was on the same sample, PMR-53, which was calibrated by ¹⁵N nuclear reaction analysis.

Comparison with the method of Paterson (1982). Values of I/γ determined in this study increase in the order garnet < clinopyroxene < orthopyroxene and are inversely correlated with the average absorption frequency of the OH-stretching vibrations in each mineral, as previously observed in other materials (Ikawa and Maeda, 1968; Paterson, 1982). However, the OH concentration of the garnet MON-9 calculated from the calibration of Paterson (1982) is 17 ppm H_2O, which is lower by a factor of three than the concentration determined in this study. The effective integrated molar absorption coefficient that corresponds to this H_2O concentration is I/γ ($=I_{eff}$) = 66440 ± 490 L/(mol·cm²) ($\gamma = 0.333$). In contrast to these values, the present study yields $I/\gamma = 20100$ L/(mol·cm²). Unfortunately, H_2O contents lower by a factor of three than those measured in garnet MON-9 would not be unambiguously distinguishable from the blank of our extraction procedure, given the present sample sizes. The OH content of the orthopyroxene, calculated from the Paterson (1982) calibration is 214 ± 55 (2σ) ppm H_2O, giving an effective integral molar absorption coefficient (I/γ) for this sample of 82200 ± 22100 (2σ) L/(mol·cm²). This is indistinguishable from the value of 80600 ± 6400 (2σ) L/(mol·cm²) determined in this study. Our calibrations confirm the order-of-magnitude appropriateness of the Paterson (1982) calibration (in contrast to some others listed above) but illustrate the importance of individual mineral calibrations for quantitative analysis of trace OH in minerals.

Applications

We expect the calibrations presented here to be rigorously applicable to pyrope-rich garnet, augitic and diopsidic clinopyroxene, and aluminous enstatite orthopyroxene with the same OH-absorption bands as the samples

analyzed in this study. The applicability to various related samples is uncertain. The fact that the IR spectrum of, for example, orthopyroxene can consist of a number of OH bands of different wavenumber (from 3600 to 3050 cm^{-1}) with different relative intensities for different samples implies that there will probably be a variation in the molar absorption coefficient that is virtually sample-specific. Ideally, it would be desirable to determine either the frequency dependence of the molar absorption coefficient for each mineral species or the molar absorption coefficient of each component band in the OH spectrum.

Most samples of pyrope garnet have broadly similar OH infrared spectra and application of the present calibration is probably generally appropriate. In addition, most diopside and augite of mantle origin show similar features in the OH-stretching region, and we suggest that the calibration may be applied to these samples with a reasonable degree of accuracy. However, caution is required in the application of the present calibration to crustal diopside because there is considerable variability in the OH spectra of such samples (see Skogby et al., 1990, Fig. 2). Furthermore, the direct application of the augite calibration to mantle-derived omphacite is questionable because of consistent spectral differences (see Skogby et al., 1990; Smyth et al., 1991). The omphacite OH spectrum is dominated by a single band at about 3450 cm^{-1}, whereas the average frequency of absorption in the augite PMR-53 is closer to 3550 cm^{-1}. An average wavenumber dependence of the absorption coefficient of 150 L/(mol·cm^3) (Paterson, 1982) predicts that the OH content of omphacite will be ~30% lower than that derived from the augite calibration. However, Skogby and Rossman (1991) determined that the dependence of I on ν for amphiboles would be five times greater than the above, illustrating that there is still considerable uncertainty in quantitative analysis of OH in omphacite.

In summary, the present calibrations should allow H determinations with uncertainties in accuracy on the order of 10–20% from high-quality OH spectra of similar band composition to those in this study. Where spectra are notably different, this uncertainty is increased by an undetermined amount, which we believe to be <50% for most upper mantle pyroxenes and garnets.

REFERENCES CITED

Aines, R.D., and Rossman, G.R. (1984a) The hydrous component in garnets: Pyralspites. American Mineralogist, 69, 1116–1126.

——(1984b) Water content of mantle garnets. Geology, 12, 720–723.
Bell, D.R., and Rossman, G.R. (1992a) Water in Earth's mantle: The role of nominally anhydrous minerals. Science, 255, 1391–1397.
——(1992b) The distribution of hydroxyl in garnets from the subcontinental mantle of southern Africa. Contributions to Mineralogy and Petrology, 111, 161–178.
Beran, A., and Zemann, J. (1986) The pleochroism of a gem quality enstatite in the region of the OH stretching frequency, with a stereochemical interpretation. Tschermaks mineralogisch-petrographische Mitteilungen, 35, 19–25.
Bigeleisen, J., Perlman, M.L., and Prosser, H.C. (1952) Conversion of hydrogenic materials to hydrogen for isotopic analysis. Analytical Chemistry, 24, 1356.
Deloule, E., France-Lanord, C., and Albaréde, F. (1991) D/H analysis of minerals by ion probe. In H.P. Taylor, J.R. O'Neil, and I.R. Kaplan, Eds., Stable isotope geochemistry: A tribute to Samuel Epstein, p. 53–64. Geochemical Society Special Publication 3, The Geochemical Society, San Antonio, Texas.
Endisch, D., Sturm, H., and Rauch, F. (1994) Nuclear reaction analysis of hydrogen at levels below 10 at.ppm. Nuclear Instruments and Methods in Physics Research B, 84, 380–392.
Epstein, S., and Taylor, H.P., Jr. (1970) The concentration and isotopic composition of hydrogen, carbon and silicon in Apollo 11 lunar rocks and minerals. Proceedings of the Apollo 11 Lunar Science Conference, 2, 1085–1096.
Frey, F.A., and Prinz, M. (1978) Ultramafic inclusions from San Carlos, Arizona: Petrologic and geochemical data bearing on their petrogenesis. Earth and Planetary Science Letters, 38, 129–176.
Gurney, J.J., Jakob, W.R.O., and Dawson, J.B. (1979) Megacrysts from the Monastery Mine. In F.R. Boyd and H.O.A. Meyer, Eds., The mantle sample: Inclusions in kimberlites and other volcanics, p. 227–243. American Geophysical Union, Washington, DC.
Ikawa, S.-I., and Maeda, S. (1968) Infrared band intensities of the stretching and librational bands of H$_2$O, D$_2$O and HDO in solids. Spectrochimica Acta, 24A, 655–665.
Ingrin, J., Latrous, K., Doukhan, J.C., and Doukhan, N. (1989) Water in diopside: An electron microscopy and infrared spectroscopy study. European Journal of Mineralogy, 1, 327–341.
Kuhn, D., Rauch, F., and Baumann, H. (1990) A low-background detection system using a BGO detector for sensitive hydrogen analysis with the ^{1}H(^{15}N,$\alpha\gamma$)^{12}C reaction. Nuclear Instruments and Methods in Physics Research B, 45, 252–255.
Kurosawa, M., Yurimoto, H., Matsumoto, K., and Sueno, S. (1992) Hydrogen analysis of mantle olivine by secondary ion mass spectrometry. In Y. Syono and M. Maghnani, Eds., High-pressure research: Applications to Earth and planetary sciences, p. 283–287. Terra Scientific, Tokyo, Japan.
Kurosawa, M., Yurimoto, H., and Sueno, S. (1993) Water in Earth's mantle: Hydrogen analysis of mantle olivine, pyroxenes and garnet using SIMS, p. 839–840. 24th Lunar and Planetary Science Conference Abstracts, Houston, Texas.
Mackwell, S.J., Kohlstedt, D.L., and Paterson, M.S. (1985) The role of water in the deformation of olivine single crystals. Journal of Geophysical Research, 90, 11319–11333.
Mathez, E.A. (1987) Carbonaceous matter in mantle xenoliths: Composition and relevance to the isotopes. Geochimica et Cosmochimica Acta, 51, 2339–2347.
Morimoto, N., Fabries, J., Ferguson, A.K., Ginzburg, I.V., Ross, M., Seifert, F.A., Zussman, J., Aoki, K., and Gottardi, G. (1988) Nomenclature of pyroxenes. American Mineralogist, 73, 1123–1133.
Newman, S., Stolper, E.M., and Epstein, S. (1986) Measurement of water in rhyolitic glasses: Calibration of an infrared spectroscopic technique. American Mineralogist, 71, 1527–1541.
Nixon, P.H., and Boyd, F.R. (1973) The discrete nodule (megacryst) association in kimberlites from northern Lesotho. In P.H. Nixon, Ed., Lesotho kimberlites, p. 67–75. Lesotho National Development Corporation, Maseru, South Africa.
Paterson, M.S. (1982) The determination of hydroxyl by infrared absorption in quartz, silicate glasses and similar materials. Bulletin de Minéralogie 105, 20–29.
Pawley, A.R., McMillan, P.F., and Holloway, J.R. (1993) Hydrogen in

stishovite, with implications for mantle water content. Science, 261, 1024–1026.

Phillips, M.W., Popp, R.K., and Clowe, C.A. (1988) Structural adjustments accompanying oxidation-dehydrogenation in amphiboles. American Mineralogist, 73, 500–506.

Rossman, G.R. (1988) Vibrational spectroscopy of hydrous components. In Mineralogical Society of America Reviews in Mineralogy, 18, 193–206.

——— (1990) Hydrogen in "anhydrous" minerals. Nuclear Instruments and Methods in Physics Research B, 45, 41–44.

Rossman, G.R., and Aines, R.D. (1991) The hydrous components in garnets: Grossular-hydrogrossular. American Mineralogist, 76, 1153–1164.

Rossman, G.R., Rauch, F., Livi, R., Tombrello, T., Shi, C.R., and Zhou, Z.Y. (1988) Nuclear reaction analysis of hydrogen in almandine, pyrope and spessartite garnets. Neues Jahrbuch für Mineralogie Monatshefte, 4, 172–178.

Scholze, H. (1960) Über die quantitative UR-spektroskopische Wasserbestimmung in Silikaten. Fortschritte der Mineralogie, 38, 122–123.

Skogby, H., and Rossman, G.R. (1991) The intensity of amphibole OH bands in the infrared absorption spectrum. Physics and Chemistry of Minerals, 18, 64–68.

Skogby, H., Bell, D.R., and Rossman, G.R. (1990) Hydroxide in pyroxene: Variations in the natural environment. American Mineralogist, 75, 764–774.

Smyth, J.R., Bell, D.R., and Rossman, G.R. (1991) Incorporation of hydroxyl in upper mantle clinopyroxenes. Nature, 351, 732–735.

Tingle, T.N., Hochella, M.F., Jr., Becker, C.H., and Malhotra, R. (1990) Organic compounds on crack surfaces in olivine from San Carlos, Arizona and Hualalai Volcano, Hawaii. Geochimica et Cosmochimica Acta, 54, 477–485.

Vedder, W., and Wilkins, R.W.T. (1969) Dehydroxylation and rehydroxylation, oxidation and reduction of micas. American Mineralogist, 54, 482–509.

Appendix 1. Uncertainties

Spectral baselines

In order to test the uncertainties involved in choice of background, the baseline for garnet was determined in three different ways. The results for five different fragments of MON-9 using the three different subtraction methods are shown in Appendix Table 1. The method judged most accurate was that which involved computer subtraction of a dehydrated sample of MON-9 and integration of the residual spectrum between 3750 and 3250 cm^{-1} (Method 1 in Appendix Table 1). These operations were performed interactively using the Nicolet FTIR control software package. Although the exact positioning of the background spectrum to be subtracted is subjective, this method is also the most reproducible of the three.

Method 2, which produced comparable precision ($\sigma = 1.8\%$) but a slightly lower mean value (although within 2σ of the above method), involved fitting the baseline by eye and calculating the integrated absorbance by carefully cutting out the printed spectrum and weighing the area representing the difference between

Appendix Table 1. Comparison of calculated absorbances and integrated absorbances for garnet sample MON-9 using three different methods

	Measurement error (%)	Absorbance per cm	Integrated absorbance per cm
Method 1	0.34	1.119 ± 0.007	77.37 ± 1.30
Method 2	1.07	1.106 ± 0.014	75.32 ± 1.38
Method 3			69.68 ± 1.58

Note: uncertainties quoted represent one standard deviation (s.d.) of the mean of five measurements, each one on a different fragment of garnet. The measurement error is 1 s.d. of the mean of ten repeated measurements on the same spectrum.

the hydrous and anhydrous garnet spectra. This method can also introduce systematic errors in accuracy because of subjective preferences of different individuals. The overall precision to be expected from this method depends on the characteristics of the spectrum and the individual preferences involved. In unfavorable cases, errors of a few tens of percent may be expected.

Method 3, deemed least accurate, was a least-squares computer fit to the spectrum, modeling the baseline as a third-order polynomial and the OH bands as a combination of six Gaussian peaks. While this method achieved extremely good fits to the sample spectra, the resulting sum of Gaussian areas is lower than the first method by about 10%, with $\sigma = 2.3\%$, and the calculated baseline does not match the spectrum of dehydrated garnet very well.

Overall uncertainties

Appendix Table 2 lists the precision with which each parameter is determined during the analysis, expressed as σ/u, in percent. Note that this does not necessarily correspond to an uncertainty in the accuracy of the parameter in question.

Appendix Table 2. Percent uncertainties

Parameter	Garnet	Clino-pyroxene	Ortho-pyroxene
Density	0.19	0.25	0.26
Sample thickness	0.1	0.2	0.2
Integrated absorbance (untreated)	1.7	3.6	3.3
Integrated absorbance of extracted OH	1.7*	3.6	3.9*
Total linear absorbance**	0.65	2.7	2.3
Sample mass	0.1	0.1	0.1
Extracted H$_2$ V	1	1	1
OH concentration	9.9*	2.8	0.75
ϵ, ϵ'	9.9	3.9	3.0
I, I'	10	4.5	4.0

* Parameters subject to uncertainty in accuracy that may be considerably greater than the precision of analysis. Reasons are discussed in the text.
** Stipulation of contributing bands required.